J Solid State Electrochem (1998) 2: 162–169

ORIGINAL PAPER

V. Radmilović · K.I. Popov · M.G. Pavlović
A. Dimitrov · S. Hadži Jordanov

The mechanism of silver granular electrodeposits formation

Received: 21 April 1997 / Accepted: 18 September 1997

Abstract Granules as a possible form of metal electrodeposit can be formed during deposition of metals, such deposition processes being characterized by large exchange current density values. Because of this, zero nucleation zones around growing grains are formed, permitting granular metal growth. In some cases of prolonged deposition, macro-crystalline deposits can be formed as well as granular ones, e.g. in the case of silver deposition at overpotentials lower than the critical value for dendrite growth initiation. The mechanism of granular deposit growth as a final form of metal electrocrystallization is proposed. Silver boulders were deposited on platinum and silver substrates. At low deposition potentials, various crystallographic forms, some of them ideal or derived from cube-octahedron-type morphology, were obtained as a result of independent grain growth inside zones of zero nucleation. In addition to cube-octahedra, twinned and multiply twinned silver particles were also observed. The nucleation density was found (1) to increase with increasing deposition overpotential, (2) to decrease with increasing silver concentration, and (3) to be greater on Ag than on Pt for the same deposition overpotential and dendrite precursors. Increasing overpotential leads to increase of density of twinned grains. The grain growth at greater overpotentials from more concentrated solution is less ideal, producing a granular deposit on prolonged deposition.

Key words Silver · Electrodeposition · Morphology · Mechanism · Granular

V. Radmilović (✉) · K.I. Popov
Faculty of Technology and Metallurgy,
University of Belgrade, Karnegijeva 4, Belgrade, Yugoslavia

M.G. Pavlović
ICTM, Department of Electrochemistry,
University of Belgrade, Njegoševa 12, Belgrade, Yugoslavia

A. Dimitrov · S. Hadži Jordanov
Faculty of Technology and Metallurgy,
University "St. Cyril & Methodius", R. Bošković 16,
Skopje, Republic of Macedonia

Introduction

Morphology is probably the most important property of electrodeposited metals. It depends mainly on the kinetic parameters of the deposition process and the deposition overpotential or current density. Obviously, the morphology of electrodeposited metal depends also on deposition time, the final form of the deposit eventually being reached.

In general, metal electrodeposits can be compact and disperse. Disperse deposits can be spongy, dendritic and granular. The mechanisms of spongy and dendritic deposits formation are well known [1–5]. Granular deposits of relatively high porosity and highly developed surface area are obtained by deposition of metals in processes characterized by large exchange current density values [6–10]. In some cases they consist of grains growing independently of each other until a compact film [11] or spongy deposit is formed on these [6].

The various phenomena related to silver electrodeposition under various experimental conditions, producing different deposit morphologies (mostly dendritic), have been extensively studied. However, it is to be noted that, despite the importance of this problem, there have been, to the knowledge of the authors of this paper, no references to granular silver electrodepositon in recent years. Nevertheless, the conditions under which granular, i.e. non-dendritic, disperse deposit is reached as a final form have not yet been elucidated. The aim of this paper is to propose the mechanism of granular deposit formation as well as to study, by means of scanning electron microscopy, granular growth in silver deposition from silver nitrate solution, in order to characterize the morphology of deposited silver particles.

Experimental

Silver was deposited from 0.1 and 0.5 M $AgNO_3$ in 1.0 M $NaNO_3$ aqueous solutions onto stationary Pt- and Ag-wire electrodes

(99,9%-Aldrich) previously treated with 1:1 HNO_3. An open cell was used. Experiments were performed at (25 ± 1) °C. Doubly distilled water and analytical grade chemicals were used.

Deposition was carried out under potentiostatic conditions at 40–100 mV overpotentials. Counter and reference electrodes were of pure silver.

Various quantities of electricity (2, 20 and 60 mAh/cm^2) were passed through the cells at given overpotentials.

The morphologies of the deposits were investigated using scanning electron microscopy (SEM, JEOL T-20 microscope) at 20 kV.

Results and discussion

The silver deposits grown on a platinum substrate are shown in Fig. 1a and b and those on a silver substrate in Fig. 1c and d. In both cases, independently growing grains are formed; the nucleation rate is evidently greater on the silver than on the platinum substrate. This difference is obviously due to the fact that the metal being deposited is in one case the same as the substrate metal and in the other case not [12].

It is seen from Fig. 1a and b that the morphology of the deposit on the platinum substrate changes considerably on increase of overpotential from 40 to 60 mV. This is less pronounced in the case of the silver substrate (Fig. 1c and d). In both cases, dendritic growth starts at 70 mV as seen from Fig. 2. The nucleation rate increases with increasing overpotential and decreasing silver ion concentration, as can be seen by comparing Fig. 1c and d with Fig. 3 [12]. The critical overpotential of dendritic growth initiation increases also with increasing deposition ion concentration [13], being 120 mV in the latter case [12]. On the other hand, the more regular growing forms are obtained for conditions of lower grain density, and at larger overpotentials the number of twinned crystals strongly increases [14, 15].

Ideal silver grains were grown earlier on a platinum substrate from silver nitrate solution using the double-pulse technique [16]. A single, square potentiostatic pulse was initially superimposed on a low steady overpotential. The height and duration of the square pulse were chosen so that single-crystal nuclei were formed only in that single event. The steady overpotential was chosen sufficiently high for crystal growth to occur but lower than the overpotentials needed for formation of new nuclei. As a result, nuclei formed in the nucleation

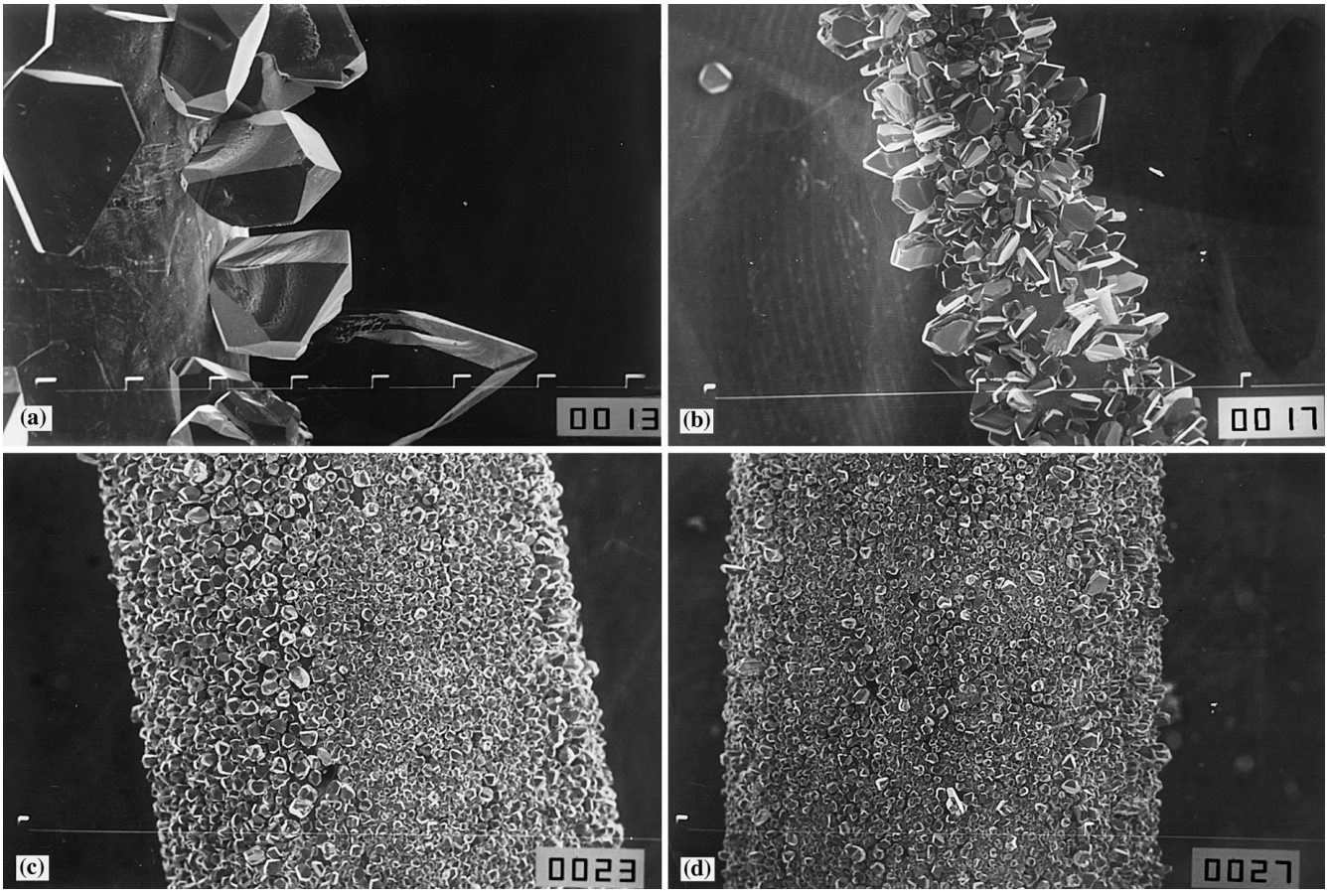

Fig. 1a–d Silver deposits obtained potentiostatically from 0.1 M $AgNO_3$ + 1.0 M $NaNO_3$ by electrodeposition onto stationary wire electrodes. Quantity of electricity 2 mAh cm^{-2}. **a, b** Platinum substrate. Magnification **a** ×200, **b** ×75. Overpotential **a** 40 mV and **b** 60 mV. **c, d** Silver substrate. Magnification ×75; overpotential **c** 50 mV and **d** 70 mV

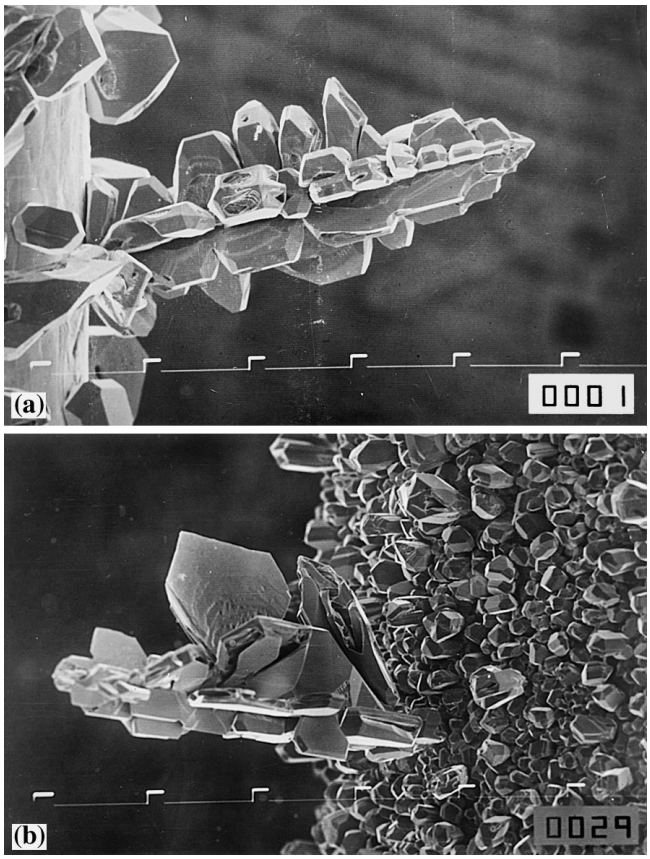

Fig. 2a, b Silver deposits obtained potentiostatically from 0.1 M $AgNO_3$ + 1.0 M $NaNO_3$ by electrodeposition onto stationary wire electrodes. Quantity of electricity 2 mAh cm^{-2}; overpotential 70 mV; magnification ×200; **a** platinum and **b** silver

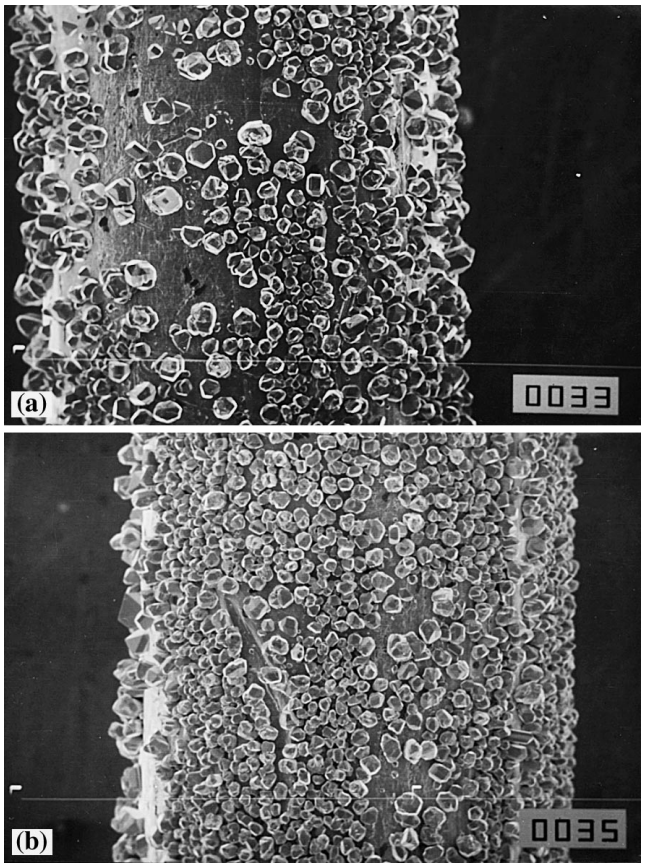

Fig. 3a, b Silver deposits obtained potentiostatically from 0.5 M $AgNO_3$ + 1.0 M $NaNO_3$ by electrodeposition onto stationary silver wire electrodes. Magnification ×75; quantity of electricity 2 mAh cm^{-2}; overpotential **a** 60 mV and **b** 80 mV

stage developed into well-defined crystal morphologies in the growth stage.

Electrolytically grown new phase centers exert a certain screening action in their near vicinity, manifested in the formation of spatial zones around them (see sketch in Fig. 4) where the nucleation process is practically arrested [17–24].

In this way the regular growth of silver grains inside the nucleation exclusion zones can be realized and the use of double-pulse technique is not necessary.

During electrodeposition, for energy reasons, some crystal morphologies appear more frequently than others. Silver crystallizes in an FCC-type lattice. Generally, an equilibrium shape of FCC particles is cube – octahedron. Some of these are clearly visible in investigated Ag particles deposited on Pt, marked A in Fig. 5a. However, many of the present particles are of a different shape, for example, twinned, such as those marked B in Fig. 5b and C in Fig. 5a and c. Some of these show a reentrant groove growth as in that marked D in Fig. 5a. Repeated one-dimensional nucleation in the groove leads to formation of flat dendrites [5], as illustrated by the dendrite precursors shown in Fig. 1b. Frequently, the crystals can take different shapes (Fig. 5d). In this case, where the Ag crystals are of the cubic type, they

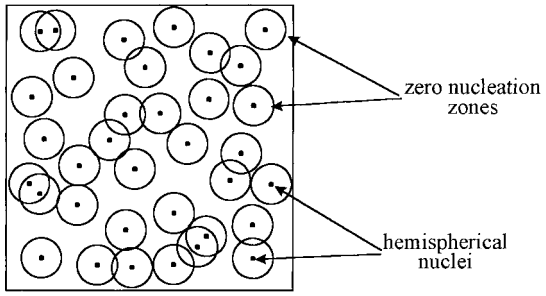

Fig. 4 Sketch of hemispherical nuclei randomly distributed on the electrode surface

may have small equilateral-triangular faces developed in place of each corner of the cube. However, at this stage of the growth, triangular-type faces in monocrystal particles are actually present.

Based on the cubic system symmetry rule, if one corner is replaced by triangular or hexagonal faces, then all eight corners will be similarly modified [25], as shown by A in Fig. 5a. The crystal then consists of six (three of which are visible) octagonal faces, which are part of the original cubic faces, and eight new equilateral triangular faces. The latter are of different forms compared to the

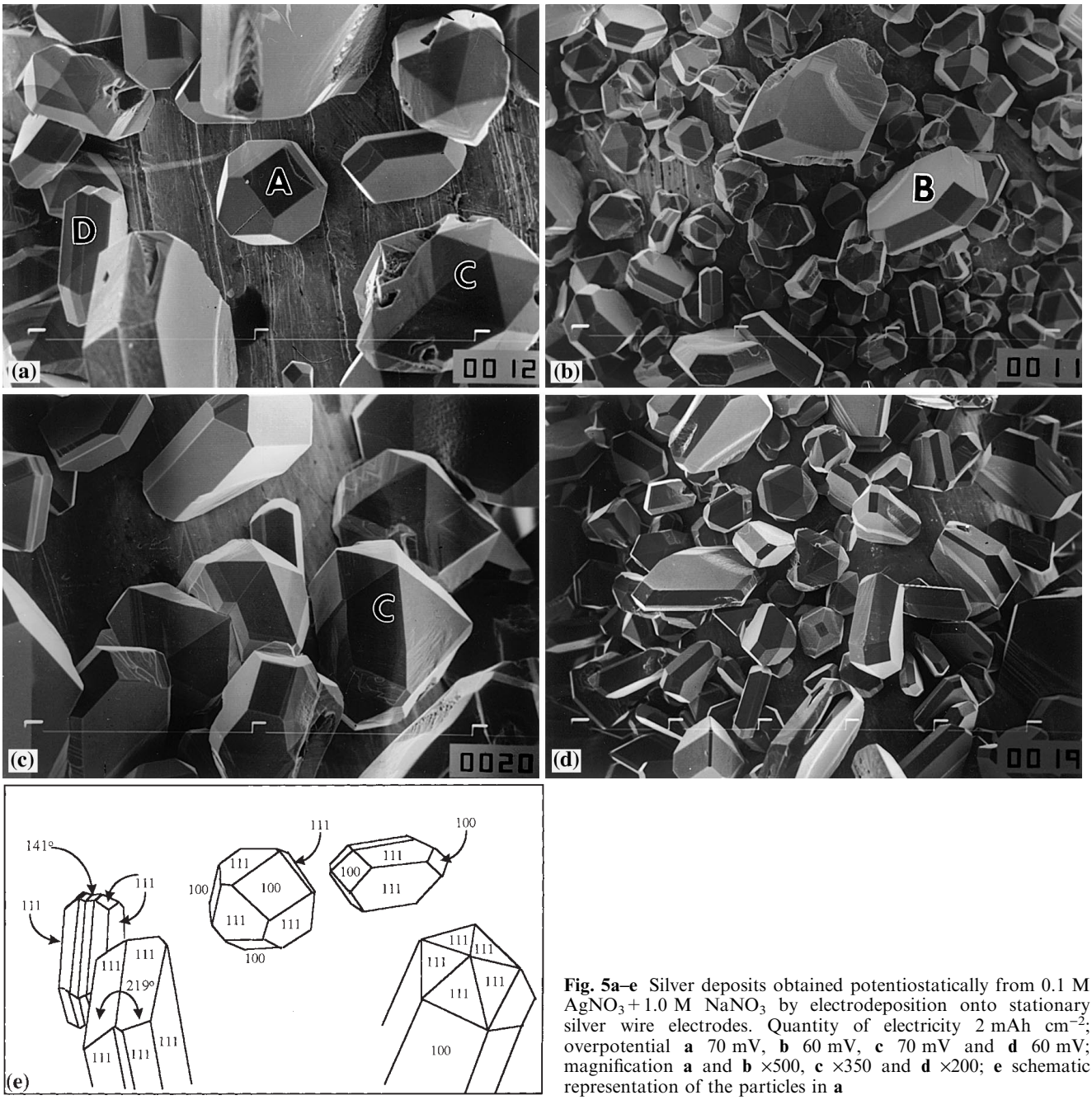

Fig. 5a–e Silver deposits obtained potentiostatically from 0.1 M $AgNO_3$ + 1.0 M $NaNO_3$ by electrodeposition onto stationary silver wire electrodes. Quantity of electricity 2 mAh cm^{-2}; overpotential **a** 70 mV, **b** 60 mV, **c** 70 mV and **d** 60 mV; magnification **a** and **b** ×500, **c** ×350 and **d** ×200; **e** schematic representation of the particles in **a**

original one. However, the assembly of faces which define the form of the crystal is always driven by the crystal symmetry. Now, the form of the Ag cubic crystal (A in Fig. 5a) is defined by two forms of the faces, six of which are of the {100} type, having a square shape, and eight are of the {111} type, developed by cutting away the original corners of the cube. How large the new triangular faces should be depends on how much the original corners are cut away. The possible shapes of the original cube can be as shown schematically in Fig. 6. The shape A in Fig. 5a is the cube-octahedron, and form E in Fig. 7a is close to a pure octahedron. It is well known that the {111} faces appear first as triangular. If the process of cutting away is continued further, the {111} faces will meet in a new set of edges and will take on a hexagonal shape (Fig. 5a).

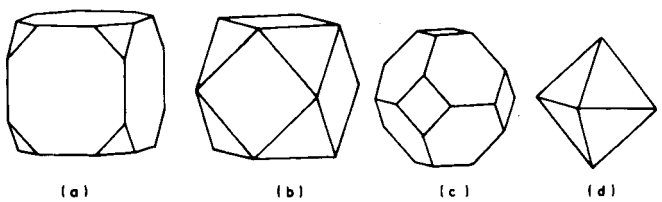

Fig. 6a–d Cubic crystal with modified corners, giving different habit: **a** initial stage, **b** and **c** cube-octahedra, **d** octahedra

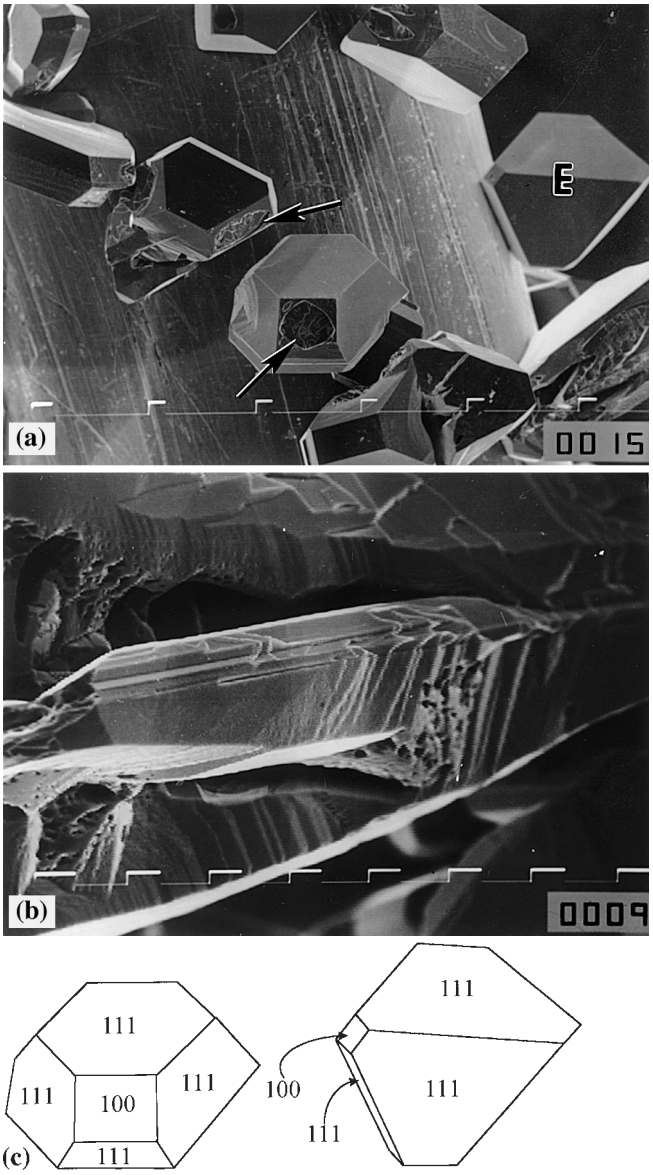

Fig. 7a–c Silver deposits obtained potentiostatically from 0.1 M $AgNO_3 + 1.0$ M $NaNO_3$ by electrodeposition onto stationary platinum wire electrodes. Quantity of electricity 2 mAh cm^{-2}; overpotential **a** 50 mV and **b** 70 mV; magnification **a** ×200 and **b** ×1500; **c** schematic representation of the particles in **a**

The final form that a given crystal will take obviously depends on the relative development of cubic and octahedral form faces. However, crystallizing the same substance (in this case silver) under different conditions, e.g. using a different the solvent, the temperature at which crystallization takes place, the presence of impurities, the deposition current density (c.d.) or overpotential, etc., leads to the same forms but in different habits, caused by varying development of different forms. Generally, for the given volume, a crystal will have the tendency to create a form with minimum surface and consequently minimum total energy. For the condition of thermodynamic equilibrium, the external form of the crystal is determined by the requirements of minimum surface free energy. This energy is the sum of the energies of all unsaturated bonds on the crystal surface, which is related to the coordination number.

For FCC silver, the surface energy will be dependent on the ratio between the number of unsaturated bonds and the coordination number 12. For example, one silver atom on the surface will contribute to the total surface energy by 1/4 of the energy for one atom, because it has three unsaturated bonds. In the ideal case, the total surface energy of the crystal will be equal to the ratio of the number of atoms occupying the faces, edges and corners to their respective numbers of unsaturated bonds [26]. Here the concept of localized bonds is assumed, i.e. the bonding forces with all but the nearest atoms are neglected.

Regardless of how the crystal has been produced in nature under a wide variety of conditions and from solutions often containing other substances as impurities, they do obey the minimum surface energy law, because the surface energy values of the faces present are modified. Hence, the cubic crystal, under certain conditions, can have all kinds of different habits which include, as well as {111} and {100} faces, also {110}, {120}, {112}, {310}, etc.

There are many examples amongst our electrodeposited Ag particles which confirm the presence of forms far away from equilibrium shapes. For example, the particles marked C in Fig. 5a and c exhibit forms which are not typical for octahedral or cube-octahedral particles [27]. These nonequilibrium shaps can be described in terms of fivefold, multiply-twinned particles (MTP's), decahedral, icosahedral, etc. It can be expected that these kinds of silver particles are stable in a certain size (nanometer range), because theoretical considerations suggest [28] that the total energy of the decahedral form is between that for a single crystal and that for an icosahedral MTP.

In many cases, surface impurities are the reason for the discrepancies between different observations on the equilibrium shapes of small particles (the presence of oxygen, and/or other atomic species). In the majority of cases, the faces seems to be flat, as are practically all the particles in Fig. 5. However, imaging some particles at a higher magnification reveals the presence of {111} close-packed plane steps (Fig. 7b). This indicates that the rate of thickening of the particles, i.e. their growth rate, is limited by the formation of ledges on {111} planes. Even when the growth rate of silver particles in our experiments is sufficiently high, the shape of the particles is still the so-called "growth shape" which is defined by the growth kinetics. We believe that the shape of the silver particles is less defined by surface energy, i.e. it does not have an "equilibrium shape". In most cases, however, the shape seems to be the result of interplay between surface energy and growth kinetics effects. Thus, the particles possibly containing {100}, {111} and {112} faces, schematically shown in Fig. 8, are also observed.

The various morphologies observed for Ag particles in electrodeposited layers can also be analyzed in terms

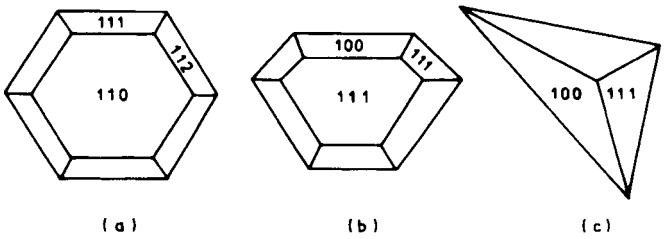

Fig. 8a–c Schematic representation of the silver particles containing {112} and {110} crystallographic faces observed in Fig. 5 viewed along different zone axes: **a** [110], **b** [111], **c** [100]

of the bicrystal symmetry. Such examples are particle D in Fig. 5a and particle B in Fig. 5b, although many of them can be described in the same fashion. The key to this behavior lies in the internal twin structure of the Ag particles. The broad faces of particle D in Fig. 5a are parallel to the {111} twin plane. In addition, this twin plane can produce a re-entrant angle (particle D in Fig. 5a) at which growth of silver particles in the ⟨211⟩ direction can take place, forming a so-called ''ribbon'' crystal. The hexagonal shape of this and similar crystals is caused by the fact that a twinned crystal is bounded only by {111} faces, forming alternatively angles 141° and 219° (see sketch in Fig. 5e). It can be shown that this particle consists of four slabs with three twinning planes parallel to each other. It is concluded that twinning plays an important role in the nucleation and growth of electrodeposited silver particles. This kind of growth is, also dendritic, and the term ''dendritic growth'' is, in fact, often used to describe a similar crystal form. However, in this case they are dendrite precursors.

By simple inspection of recorded images, it is also concluded that the {111} and {100} faces are the most prominent (see Figs. 5e and Fig. 7c), while the particles containing {112} and {110} faces, schematically shown in Fig. 8, are present less frequently. It is interesting to note that development of ''equilibrium shapes'', where dominant faces are {111} and {100}, is associated with higher grain density and concentration of electrolyte.

In most cases, however, the shape seems to be the result of interplay between surface energy and growth kinetic effects (F in Fig. 9). The ''equilibrium shape'' is certainly also affected by the electrode potentials and the particle size. It is seen from Fig. 9 that the grains obtained on a silver substrate on prolonged deposition from more concentrated solution and at larger overpotentials are less ideal than those obtained at lower overpotentials from less concentrated solutions (Figs. 1a, 5, 7a), which is in accordance with the above conclusion. It is also seen that the granular deposit is probably the final form in this case. This can be explained (see Fig. 10) in the following way.

In the initial stage of deposition, the silver nuclei are formed as well as the zero nucleation zones around them as well as the diffusion zone [29]. The initial stage of deposition is characterized by independent growth of nuclei and grains. Around them the zero nucleation

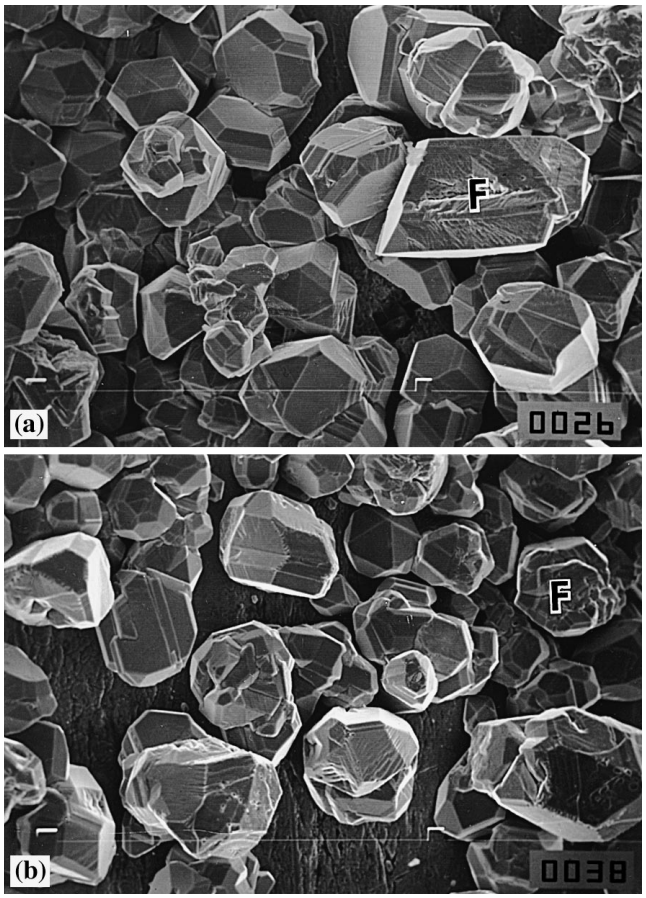

Fig. 9a, b Silver deposits obtained potentiostatically from 0.5 M $AgNO_3 + 1.0$ M $NaNO_3$ by electrodeposition onto stationary **a** platinum and **b** silver wire electrodes. Quantity of electricity 2 mAh cm^{-2}; magnification ×750; overpotentail **a** 60 mV and **b** 100 mV

zones and spherical diffusion zones are formed. The deposition rate is similar in all directions as well as the dimensions of particles (Fig. 1c and d and Fig. 3). Nucleation does not occur simultaneously over all the cathode surface but is a process extended in time so that crystals generated earlier may be considerably larger in size than those generated later (Fig. 9). An exclusion zone for further nucleation always develops around an already randomly formed nucleus. After some time, the depletion zones around the largest grains start to interfere and lateral growth is decreased. The lower grains are in the overlap field, and their growth is considerably lowered (Fig. 10a and b). In prolonged deposition around the tips of the largest protrusions, spherical diffusion takes place and these tips grow toward the bulk of solution. The growth of lower grains is completely blocked (Fig. 10). In this way, the granular deposit as a final form of silver deposition is formed.

Hence, it is necessary that the zero nucleation zone and the spherical diffusion field around the growing grains are formed at overpotentials lower than the critical overpotential of dendritic growth initiation. It seems that these conditions are fulfilled in prolonged deposition only in the case of silver. The formation of zero

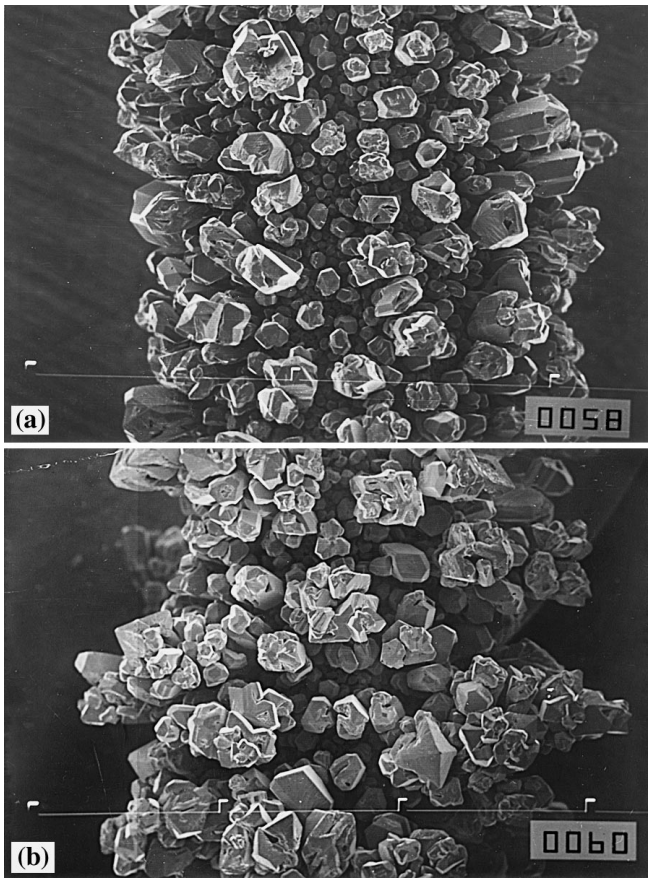

Fig. 10a, b Silver deposits obtained potentiostatically from 0.5 M $AgNO_3$ + 1.0 M $NaNO_3$ by electrodeposition onto stationary silver wire electrodes. Quantity of electricity **a** 20 mAh cm^{-2} and **b** 60 mAh cm^{-2}; overpotential **a** 60 mV and **b** 100 mV; magnification **a** ×50 and **b** ×35

nucleation and spherical diffusion zones requires a large value of the exchange current density in the deposition process. In contrast to the silver deposition process from a simple soluble salt solution, lead, tin, cadmium and zinc deposition processes from appropriate electrolyte solutions are characterized by large values of exchange current densities. The zero nucleation zone radius r is given by:

$$r = \frac{E}{E - \eta_{cr}} \qquad [1]$$

according to [1], assuming full ohmic control of the deposition process, where E is the ohmic potential and η_{cr} the crystallization overpotential. According to Klapka [30] η_{cr} depends strongly on the exchange current density of the deposition process and on the number of electrons transferred in it. The η_{cr} value decreases with decreasing j_0 and increasing z (j_0 is the exchange current density and z the number of electrons). Ag, Pb, Sn, Cd and Zn deposition processes are characterized by high j_0 values, but the critical overpotential of dendritic growth initiation is very low in the case of Pb and Sn [5], making granular growth impossible. In silver deposition, dendrites appear at larger overpotentials and η_{cr} is twice as large as in the case of Cd and Zn, meaning a considerably larger r for the same value of E. Because of this, in Cd and Zn deposition, after longer deposition times surface, films are formed as the final form of the deposit. (In the deposition of Zn from alkaline zincate solutions, the formation of spongy deposits over boulders is possible [2, 3, 6], while, in the case of silver, granules can be obtained as a final form of deposit.)

The presence of imperfections on the furthest surfaces of some silver crystals (arrowed in Fig. 7a) indicates that the supply of silver adatoms is partially from the platinum electrode, which is in agreement with Hepel et al. [31]. However, since the majority of the particles are perfect in shape with no surface defects, this indicates that the silver ions from the surrounding solution are reduced mainly on silver particle facets directly. This is confirmed by the presence of the fine 111 surface steps, observed at higher magnification (Fig. 7b).

Conclusions

1. Granules as a possible form of metal electrodeposit can be formed during deposition of metals, these deposition processes being characterized by large exchange current density values. Because of this, zero nucleation zones around growing grains are formed, permitting granular metal growth. In some cases, on prolonged deposition, macro-crystalline deposits can be formed as well as granular ones in the case of silver deposition at overpotentials lower than the critical one for dendrite growth initiation.
2. The nucleation density was found (1) to increase with increasing deposition overpotential, (2) to decrease with increasing silver concentration, and (3) to be greater on Ag than on Pt for the same deposition overpotential and dendrite precursors. Increasing overpotential leads to increase of density of twinned grains. The grain growth at greater overpotentials from more concentrated solution is less ideal, producing a granular deposit on prolonged deposition.
3. Various crystallographic forms, some of them ideal, or derivatives of cube-octahedron type morphology were obtained at low deposition overpotentials because of independent grain growth inside zones of zero nucleation. In addition to cube-octahedra, twinned and multiply twinned silver particles were observed.
4. The mechanisms of silver deposition involve three-dimensional nucleation and growth as well as deposition layer by layer of {111} close-packed planes, manifested by the presence of 111 surface steps.
5. The majority of the particles are perfect in shape with no surface defects, which indicates that silver ions from the surrounding solution are reduced predominantly on the silver particle surfaces directly. This is confirmed by the presence of the observed fine 111 surface steps.

References

1. Barton Jl, Bockris JO'M (1962) Proc R Soc London, Ser A 268: 485
2. Diggle JW, Despić AR, Bockris JO'M (1969) J Electrochem Soc 116: 1503
3. Popov KI, Krstajić NV (1983) J Appl Electrochem 13: 775
4. Despić AR, Popov KI (1972) In: Conway BE, Bockris JO'M (eds) Modern aspects of electrochemistry, No. 7, chap 4. Plenum Press, New York
5. Popov KI, Krstajić NV, Čekerevac MI (1996) In: White RE et al. (eds) Modern aspects of electrochemistry, no 30, chap 3. Plenum Press, New York
6. Bockris JO'M, Nagy Z, Dražić D (1973) J Electrochem Soc 120: 30
7. Despić AR, Dražić DM, Mirjanić MD (1978) Faraday Disc Chem Soc 12: 126
8. Jovićević JN, Despić AR, Dražić DM (1977) Electrochim Acta 22: 577
9. Jovićević JN, Dražić DM, Despić AR (1977) Electrochim Acta 22: 589
10. Popov KI, Krstajić NV, Jerotijević Z, Marinković SR (1985) Surf Technol 26: 185
11. Popov KI, Čekerevac MI, Nikolić LjN (1988) Surf Coatings Technol 34: 219
12. Dimitrov AT, Hadži Jordanovi S, Popov KI, Pavlović MG, Radmilović V J Appl Electrochem (in press)
13. Popov KI, Pavlović MG, Maksimović MD (1982) J Appl Electrochem 12: 525
14. Pangarov NA, Velinov V (1968) Electrochim Acta 13: 1641
15. Pangarov NA, Velinov V (1968) Electrochim Acta 13: 1909
16. Pangarov NA, Velinov V (1966) Electrochim Acta 11: 1753
17. Markov I, Boynov A, Toschev S (1973) Electrochim Acta 18: 377
18. Milchev A (1983) Electrochim Acta 28: 947
19. Scharifker BR, Mostany J, Serruya A (1992) Electrochim Acta 37: 2503
20. Serruya A, Mostany J, Scharifker BR (1993) J Chem Soc Faraday Trans 89: 255
21. Milchev A, Kruijt WS, Sluyters-Rehbach M, Sluyters JH (1993) J Electroanal Chem 362: 21
22. Isaev VA, Baraboshkin AN (1994) J Electroanal Chem 377: 33
23. Kruijt WS, Sluyters-Rehbach M, Sluyters JH, Milchev A (1994) J Electroanal Chem 371: 13
24. Mostany J, Serruya A, Scharifker BR (1995) J Electroanal Chem 383: 37
25. Philips FC (1971) An introduction to crystallography. Oliver and Boyd, Edinburgh, p 9
26. Romanowski W (1969) Surface Sci 18: 373
27. Jose-Yacaman M, Avalos-Borja M (1992) Catal Rev Sci Eng 34: 55
28. Marks LD (1984) Phil Mag A 49: 81
29. Sluyters-Rehbach M, Wijenberg JHOJ, Bosco E, Sluyters JH (1987) J Electroanal Chem 236: 1
30. Klapka V (1970) Collection Czechoslov Chem Commun 35: 899
31. Hepel T, Pollak FH (1988) J Electrochem Soc 135: 562